Modelling of the Blood Plasma Species of Biguanide Derivatives Exhibiting Potential as Diagnostic Radiopharmaceuticals

Judith M. Wagener[a]*, Midred K. Dithebe[a], Daniel Mogano[b], Ignacy Cukrowski[b] and Jan Rijn Zeevaart[c]

[a]*Radiochemistry, NECSA, P.O. Box 582, Pretoria 0001, South Africa.*

[b]*Department of Chemistry, University of Pretoria, Pretoria 0002, South Africa.*

[c]*CARST, North West University, Mafikeng Campus, Private Bag X2046, Mmabatho 2735, South Africa.*

ABSTRACT

^{99m}Tc-DMSA (DMSA=dimercaptosuccinic acid), the gold standard for static renal imaging, has a long uptake time, which is a limiting factor in diagnostic procedures and also leads to a relatively high radiation dose to patients. The ligands dimethyl biguanide (DMBG), biuret (BIU), 2-imino-4-thiobiuret (ITB) and carboxy-biguanide (CBIG) have nitrogen donor atoms, which are able to complex transition elements. The formation constants needed in order to establish a blood plasma model for these ligands were determined by potentiometry and the results are reported herein. Based on blood plasma modelling, it was shown that the ligands had selectivity for ^{99m}Tc over blood plasma metal ions at physiological pH and it was therefore hypothesized that the Tc-ligand complex would survive in blood plasma. Furthermore, no or few side effects related to the mobilization of blood plasma metal ions by these ligands are expected, once the radiopharmaceutical has been administered. It is also expected that these ligands should clear rapidly from the blood plasma.

1. Introduction

In the field of diagnostic radiopharmaceuticals, a number of successful ^{99m}Tc-based radiopharmaceuticals are available in the market, because of the availability of ^{99m}Tc from generators on demand. Furthermore, its half-life (6 h) and 140 keV gamma rays make it the almost ideal isotope for imaging of biological processes. Many ^{99m}Tc-based radiopharmaceuticals were designed in the 1980s and 1990s, one area being kidney diagnostic agents.[1]

^{99m}Tc-radiopharmaceuticals are used for static renal imaging that provides morphological information on each kidney. ^{99m}Tc-DMSA is an imaging agent which is fixed in the proximal renal tubular cells. This radionuclide complex is extracted from the blood by the renal tubular cells, but is not excreted into the tubuli.[2,3] The low urine excretion and time delay prior to scintigraphy led to the development of new ^{99m}Tc agents that permit rapid imaging with lower radiation doses to the patient.[4] ^{99m}Tc-DMBG showed distinct renal and urinary excretion profiles in rabbits, cleared faster and showed better contrast in the whole-body images, with the same acquisition times as ^{99m}Tc-DMSA.[5] According to the literature, ^{99m}Tc-BIG has promising practical and dosimetric features as an alternative renal imaging agent to ^{99m}Tc-DMSA.[4–6] The simultaneous recording of morphological and functional data was possible.

The ^{99m}Tc complexes with dimethyl biguanide (DMBG), biuret (BIU), 2-imino-4-thiobiuret (ITB) and carboxy-biguanide (CBIG) (see Fig. 1) show potential, on theoretical grounds, as alternative kidney-imaging agents for ^{99m}Tc-DMSA. Biguanide (BIG) and its N-substituted derivates are bidentate ligands with nitrogen donor atoms and can act as bidentate donors that are able to coordinate transition metals.[6] Carboxy-biguanide (CBIG) is a substituted biguanide with a propanoic acid group attached at the N^1 position. It is postulated to form a $[TcO(BIG\text{-}COO)_2]^-$ complex, as opposed to a $[TcO(BIG)_2]^+$ complex, which could assist in its clearance from the kidneys. It is possible to consider that biguanide is derived from the substitution of both oxygen atoms of biuret by imino (=NH) groups.[7] ITB is similar to biguanide but one amidine group is replaced with a sulphur atom. These compounds are strong σ- and π-donating ligands that form stable complexes with transition metal ions in high or usual oxidation states, utilising the availability of vacant d orbitals of the metal that may overlap with the filled π orbitals of the ligand. The metal ions are coordinated through the two imino groups.[8]

Biguanides have demonstrated antidiabetic characteristics by reducing glucose production in the liver, improving insulin sensitivity as well as antiobesity effects. Various biguanide derivatives have been evaluated for retaining antidiabetic activity and maintaining resistance to creatine-like metabolism that should make them less prone to muscle accumulation.[9]

Our group has recorded some success in using blood plasma models in predicting and describing potential bone-seeking agents (bisphosphonates).[10–12] Most of the agents screened by this *in vitro/in silico* technique were found not to have potential and their drawbacks were indicated. These were then proven by selected animal tests. The models could also elucidate the *in vivo* behaviour found. Although the model has thus far not predicted improved bone-seeking radiopharmaceuticals, its success lies in the faster screening of agents and in avoiding excessive animal testing. The use of a thermodynamic model alone has some obvious constraints, but makes sense, if one considers that

* To whom correspondence should be addressed. E-mail: jwagener@necsa.co.za
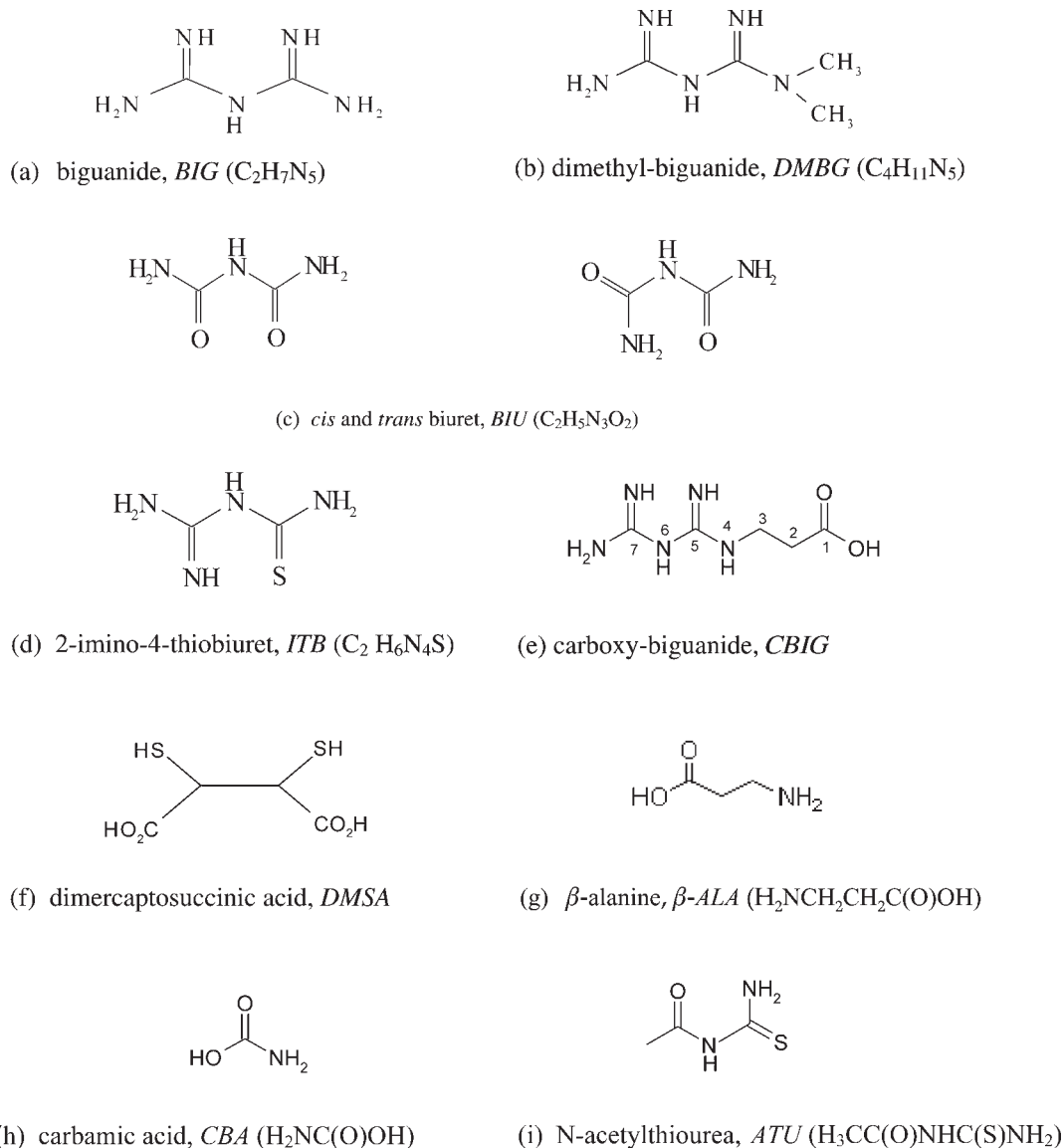
(a) biguanide, *BIG* ($C_2H_7N_5$)

(b) dimethyl-biguanide, *DMBG* ($C_4H_{11}N_5$)

(c) *cis* and *trans* biuret, *BIU* ($C_2H_5N_3O_2$)

(d) 2-imino-4-thiobiuret, *ITB* ($C_2 H_6N_4S$)

(e) carboxy-biguanide, *CBIG*

(f) dimercaptosuccinic acid, *DMSA*

(g) β-alanine, *β-ALA* ($H_2NCH_2CH_2C(O)OH$)

(h) carbamic acid, *CBA* ($H_2NC(O)OH$)

(i) N-acetylthiourea, *ATU* ($H_3CC(O)NHC(S)NH_2$)

Figure 1 Structures of the ligands.

radiopharmaceuticals are often metal-based with an organic ligand being the carrier of the radioactive labelled metal ion to the target. In the screening of a potential agent, the formation constants for the ligand-metal ion interaction are determined, including the interactions of the ligands with the blood plasma metal ions Ca(II), Mg(II) and Zn(II) by using ESTA (Equilibrium Simulation by Titration Analysis),[13] while the constants describing the metal ion interaction with the 40 blood plasma ligands were obtained from ECCLES (Evaluation of Constituent Concentration in Large Equilibrium Systems).[14] By now, several metal ions have been included in the model and even more constants for these complexes can be found in the literature. All these constants were incorporated into the model and the speciation of the proposed metal-ligand systems (at certain concentration) was computed. From the results, one can deduce several things, for instance whether the complex remains intact in the blood plasma or the species forming at a blood pH of 7.4 are neutral and could therefore be 'filtered' by the liver. For the work described in this publication, the same approach was attempted, although the formation constants for Tc itself could not be measured and one had to rely on the ligand interaction with other blood plasma metal ions. It is well known that Tc has many oxidation states and the determination of the formation

constants between Tc and ligands is therefore very difficult. Furthermore, there are no stable isotopes of Tc, although [99g]Tc (long-lived beta-emitter forms from the decay of the metastable ^{99m}Tc, which is the short-lived gamma-emitting nuclear isomer, by gamma emission) has a half-life of 211 000 years and could, in principle, be used; however, the long half-life makes working with this isotope a high contamination risk. It is therefore not surprising that only a few formation constants are available in the NIST database.[15] Although one can use the linear free energy relationship (LFER) plots to estimate formation constants of an unknown metal ion,[11] one needs a few reliable formation constants to compare with other metal ions. Not one of the formation constants for Tc (including for hydroxide) meets the criteria for the NIST database.[15] This implied that the LFER technique was not a possible option. However, if one considers that ^{99m}Tc is no-carrier-included (referring to the fact that only radioactive ^{99m}Tc metal ions are included in the preparation without non-radioactive isotopes as carrier),[16] the amount of Tc is between 0.2 and 1 nmol per injected dose, while the corresponding amount of ligand is 5.5 μmol. This implies that the number of Tc metal ions injected is minute (one Tc atom per 5500 to 27500 DMSA molecules), which led us to believe that one could approach the blood plasma modelling without the

Tc-ligand formation constants. One would simply measure the constants of the ligand with the main blood plasma metal ions, as well as the Sn(II) (which is normally included in the formulations as a reducing agent), and see whether there is a significant binding of blood plasma metal ions to the ligand. If this is not the case, one can assume that the Tc-ligand complex stays intact when introduced in the blood plasma. This differs from the normal quality control carried out on radiopharmaceuticals where one tests whether the complex stays intact in a solution, normally ethanol. In the blood plasma model, the Tc-ligand complex is mixed with the 40 other ligands that constitute blood plasma, to see how the competition of these ligands affects the complex.

The complexation of the ligands DMBG, BIU, ITB and CBIG with blood plasma metal ions at physiological pH 7.4 was therefore investigated.

2. Materials and Methods

2.1. Reagents

All reagents used were of analytical grade. Fresh metal ion solutions were employed in the titrations. These were made by dissolving chloride salts of the metal ions in distilled water, followed by standardization by complexometric titration using EDTA and a Metrohm Titrino equipped with a copper selective electrode. Where necessary, solutions were acidified to prevent hydrolysis. The ligands BIU, DMSA, DMBG and ITB were obtained commercially from Sigma-Fluka and Sigma-Aldrich (Johannesburg, South Africa) while CBIG was prepared as documented elsewhere.[17]

2.2. Potentiometry

Titrations were performed using a Metrohm Titroprocessor 670 with Metrohm 665 Dosimat and a Metrohm combination glass electrode (6.0222.100 Ag/AgCl reference). The glass electrode was calibrated using strong acid-base titration data. Plausible correlation was found with previous determinations of protonation constants of serinate and the literature (see Supplementary Material). The reaction solutions were contained in a jacketed vessel through which the water at 25.0 ± 0.1 °C was circulated from a Grant W14 (Johannesburg, South Africa) thermostat bath. All the titrations were performed in an inert atmosphere (by purging the solutions with nitrogen gas the mixtures were kept carbon-free) and at a constant ionic strength of 0.15 mol dm^{-3} NaCl. All solutions were prepared using distilled, de-aerated water and kept under nitrogen.

Titrations were performed, beginning at low and ending at high pH values, by the addition of 0.05 mol dm^{-3} NaOH in 0.1 mol dm^{-3} NaCl solution (solution bottle fitted with calcium oxide trap to ensure that it stayed carbon-free). Protonation constants were calculated from the data obtained from titration at different ligand-acid ratios, varying from 1:1 to 1:3. The apparent formation constants were calculated from titration data at different metal:ligand ratios. Data were analysed with the ESTA library of programs. The determined protonation constants, hydrolysis constants and pK_w from the literature[15] were held constant during optimization procedures. Experimental and calculated formation and protonation constants were compared to verify the plausibility of the model.

2.3. Polarographic Titrations

Polarographic experiments (DC$_{TAST}$) were performed for L$_T$:M$_T$ ratios from 20 to 158 for the Zn-CBIG system (ligand titrations). This ligand titration approach was adopted as a result of the

initial modelling, indicating the possibility of the formation of a precipitate at a pH of about 8. A polarographic DC wave for the free metal ion was recorded at a pH of about 5. Ligand titrations resulted in a small change in pH (about 0.7 pH units). All measurements were performed at an ionic strength of 0.15 mol dm^{-3} NaCl and an initial total metal ion concentration of 1.270 × 10^{-4} mol dm^{-3}.

2.4. Blood Plasma Modelling

The ECCLES (Evaluation of Constituent Concentrations for Large Equilibrium Studies) program was used for speciation calculations in this paper. The model itself[14] as well as its use by our group[10-12] are well documented and the functioning of the model therefore falls outside the scope of this publication. The ECCLES formation constant database was updated to include formation constants for the biguanide-type ligands and DMSA with the blood plasma metal ions Ca(II), Mg(II) and Zn(II) determined in this study. The concentrations used to model the metal ion ligand complex in blood plasma were based on the expected amounts of the individual compounds that would be present in blood after injection of a standard formulation of these ^{99m}Tc-labelled compounds. The volume of blood in a monkey was estimated to be 60 cm^3 per kg body mass and the average mass of the vervet monkeys was 6 kg. A blood volume of 360 cm^3 was assumed and the concentration of ligand in blood plasma was calculated to be 5.0 × 10^{-5} mol dm^{-3} for DMBG, 7.3 × 10^{-5} mol dm^{-3} for BIU, 6.3 × 10^{-5} mol dm^{-3} for ITB, 4.3 × 10^{-5} mol dm^{-3} for CBIG and 1.4 × 10^{-5} mol dm^{-3} for DMSA. For the modelling of the Sn(II)-DMBG complex, a concentration of 1.9 × 10^{-4} mol dm^{-3} for Sn(II) was used in addition to the DMBG. The corresponding free Sn(II) concentration was 1.6 × 10^{-5} mol dm^{-3}. Part of the output of the ECCLES program is the plasma-mobilizing index (p.m.i.). This is defined as the ratio of the total concentration of low-molecular-mass (l.m.m.) species of the metal ion after addition of the species to blood plasma to the total concentration of l.m.m. complexes before addition.

$$\text{p.m.i.} = \frac{\text{total l.m.m. metal ion concentration in the presence of the agent}}{\text{total l.m.m. concentration in normal plasma}}$$

The p.m.i. values give an indication of which blood plasma metal ions are mobilized by the added ligand (which will act as a drug). For reasons stated earlier, no formation constants for Tc were included and the assumption was made that the complex is strong and that one only needs to consider the interaction of the ligand with the blood plasma metal ions.

3. Results and Discussion

3.1. Potentiometry

The modelling results for the studied ligand systems using ESTA are given in Table 1. In all the systems investigated, the standard deviations obtained for the formation constants as well as the Hamilton R-factor were low and the calculated and experimental curves followed each other satisfactorily, providing confidence with regard to the models chosen. Protonation, formation and deprotonation curves not discussed are available from the corresponding author on request.

3.1.1. *Protonation of DMBG*

The $\bar{Z}_H$-curves shown (as an example) in Fig. 2 show inflections at $\bar{Z}_H = 1$ (pH 4) and as $\bar{Z}_H$ (protonation formation function; the average number of protons per ligand) approaches 2 (pH<2), which indicate formation of the LH and LH$_2$ species, respectively. It is, however, important to note that in the pH 4 to 10

Table 1 Measured protonation and formation constants at 25 °C and 0.15 mol dm^{-3} NaCl total ionic strength.

Equilibrium	Log K				
	DMBG	BIU	ITB	CBIG	DMSA
L + H = LH	11.52 ± .01	11.83 ± 0.01	5.73 ± 0.01	4.04 ± 0.002	9.73 ± 0.02
LH + H = LH$_2$	2.97 ± 0.01			2.55 ± 0.005	4.73 ± 0.02
LH$_2$ + H = LH$_3$					2.94 ± 0.03
Hamilton R-factor	0.0042	0.0042	0.0268	0.00451	0.0361
Data points	291	374	600	600	353
Mg + L + OH = MgLOH			5.92 ± 0.03		
Mg + L = MgL	3.10 ± 0.02	4.13 ± 0.01	2.36 ± 0.04		6.82 ± 0.03
Mg + L + H = MgLH				7.41 ± 0.02	
MgLH + H = MgLH$_2$				2.91 ± 0.04	
2Mg + L = Mg$_2$L					11.11 ± 0.06
2MgL + H = Mg$_2$LH					5.80 ± 0.06
Hamilton R-factor	0.0078	0.0097	0.0281	0.02194	0.01587
Data points	381	374	309	317	155
Ca + L + OH = CaLOH			5.43 ± 0.01		
Ca + L = CaL	3.02 ± 0.02	3.71 ± 0.01			7.31 ± 0.04
Ca + L + H = CaLH				6.90 ± 0.04	
CaLH + H = CaLH$_2$				2.81 ± 0.06	
2Ca + L = Ca$_2$L					–12.46 ± 0.06
2CaL + H = Ca$_2$LH					5.22 ± 0.06
Hamilton R-factor	0.0051	0.0039	0.0231	0.01738	0.01573
Data points	357	368	300	317	106
Ni + 2L + 2OH = NiL$_2$OH$_2$			19.14 ± 0.01		
Hamilton R-factor			0.0108		
Data points			190		
Cu + L + 2OH = CuLOH$_2$					20.64 ± 0.04
Cu + L + OH = CuLOH				13.36 ± 0.007	14.38 ± 0.04
Cu + L = CuL					7.24 ± 0.05
2Cu + L = Cu$_2$L					11.58 ± 0.07
Cu$_2$L + H = Cu$_2$LH					5.13 ± 0.09
Hamilton R-factor				0.02204	0.01834
Data points				327	165
Zn + L + = ZnL	12.57 ± 0.01	12.79 ± 0.02		7.19 ± 0.01	
Zn + 2L + 2OH = ZnL$_2$OH$_2$			17.04 ± 0.02		
Hamilton R-factor	0.012	0.017	0.0268		
Data points	377	341	337		
Sn + L + OH = SnLOH	20.91 ± 0.07				
Hamilton R-factor	0.078				
Data points	330				

range only the LH species is present. The results are comparable with the values reported by Sarma and Ray of 12.40 and 3.24, considering that the experiment was performed at different experimental conditions of 20 °C and 0.5 mol dm^{-3} ionic strength *vs.* 25 °C and 0.15 mol dm^{-3} NaCl ionic strength used in our experiments.[15] Since the protonation constants are so far apart, small uncertainties in these values will have no impact on the modelling at pH = 7.4.

3.1.2. *Protonation of BIU*

The $\overline{Z}_H$ curves (not shown) with $\overline{Z}_H = 1$ indicate the predominance of the LH species over the pH range 2–11. The second proton is lost at pH values outside those used in the glass electrode potentiometric measurements. According to Sanyal *et al.*, both amide protons are simultaneously liberated at higher pH with only one protonation constant (pH > 10.5) found.[18] However, during this work, the simultaneous liberation of both amide protons was not observed.

3.1.3. *Protonation of ITB*

The inflection at $\overline{Z}_H = 1$ up to pH 5 indicates that one proton is bound to the ligand in this pH region and corresponds to LH found with the model. At pH = 7.4 ($\overline{Z}_H = 0$) the L species will therefore predominate.

ITB has almost the same structure as biguanide, except that one imine group is replaced by sulphur. The thiol group is a weak acid (pK usually between 9 and 10), but it binds strongly to soft metal ions.[19] Therefore, the second protonation formation

Table 2 Protonation and formation constants from literature[15] for ligand analogues.

Equilibrium	BIG	CAB	ATU	B–ALA
L + H = LH	13.00	–1.18	5.73 [a]	10.08
L + 2H = LH$_2$	16.01			13.59
Cu + L + H = CuLH	11.69	–	11.53	12.03[b]
Cu + 2L = CuL$_2$	21.3	–	–	7.08
Cu + 3L = CuL$_3$	–	–	12.75	12.6
Cu + 4L = CuL$_4$	–	–	13.81	–
Zn + L = ZnL	–	0.5	–	4.10
Zn + 2L = ZnL$_2$	–	0.8	–	8.0 [b]
Zn + 3L = ZnL$_3$	–	0.9	–	10.4 [b]
Ni + L = NiL	–	–	–	4.54
Ni + 2L = NiL$_2$	16.1	–	–	7.87
Ni + 3L = NiL$_3$	–	–	–	9.7
Cd + L = CdL	–	1.3	–	–

[a] The protonation constant for ITB was used, as the protonation constant for ATU in the NIST database is listed as non-critical.
[b] The formation constants were measured at different ionic strengths from 0.1 mol dm^{-3}.

constant from one of the amide protons is lowered to an undetectable value, outside the pH values used in the glass electrode potentiometric measurements, and the first constant to 5.73, in comparison with the two pK$_a$ values of 11.52 and 2.97 found for DMBG.

3.1.4. *Protonation of CBIG*

The protonation curves (not shown) indicate that protons are lost by the ligand at pH 2.5 ($\overline{Z}_H$ approaching 2) and 4 ($\overline{Z}_H \approx 1$) and that, from pH 6 ($\overline{Z}_H = 0$) onwards, no further protons are lost, meaning that L predominates at physiological pH. A proton is probably lost beyond pH 11, which fell outside the pH range studied. The proton lost at low pH comes from the carboxylic acid followed by a proton from one of the two amidine groups.

3.1.5. *Protonation of DMSA*

The protonation curves (not shown) indicate that the third proton was lost at pH > 11. The calculated and the experimental data points approach a $\overline{Z}_H$ value of 3 at lower pH values, confirming that there are three dissociable protons for DMSA. The curves show slight inflections at $\overline{Z}_H = 2$, pH = 3.5 and at $\overline{Z}_H = 1$ from pH 5.5 to pH 9.5, confirming the LH$_2$ and LH species. This means that HL predominates at physiological pH. At pH 10.5, the curves stabilize at about $\overline{Z}_H = 0$, indicating that no further protons are lost by the ligand in this pH range. The protonation constants compare reasonably well with the literature values, considering that the temperature and ionic strength in this study differ from those employed in the literature (see Table 2).[15]

Metal–Ligand Systems
3.1.6. *Mg(II), Ca(II)-DMBG, BIU, ITB and CBIG Systems*

The alkaline earth metals Ca(II) and Mg(II) react with DMBG and BIU, showing similar $\overline{Q}$ (deprotonation function: the average number of protons released on complexation per metal ion) and $\overline{Z}_M$ (formation function: the average number of ligands per metal ion) curves. The $\overline{Z}_M$ curves show a tendency to move to
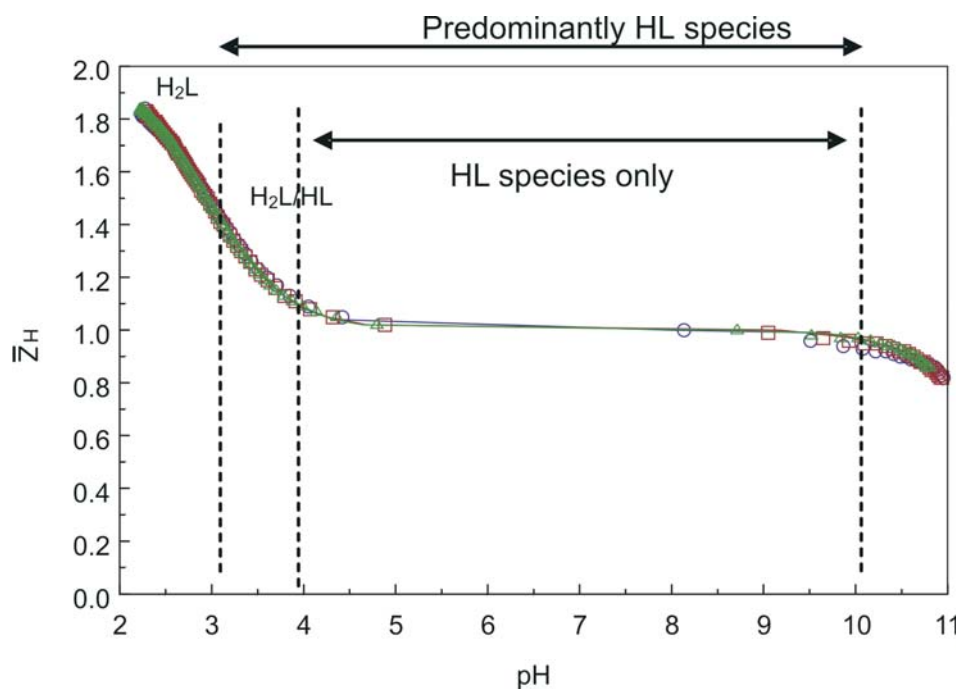

Figure 2 Experimental (symbols) and modelled (lines) protonation formation curves for DMBG. The titrations are represented by: (○) 0.001001 mol dm^{-3} DMBG and 0.011013 mol dm^{-3} HCl; (□) 0.002002 mol dm^{-3} DMBG and 0.012014 mol dm^{-3} HCl; (△) 0.003003 mol dm^{-3} DMBG and 0.012990 mol dm^{-3} HCl; *versus* 0.0500 mol dm^{-3} NaOH in 0.10 mol dm^{-3} NaCl at 25 °C and 0.15 mol dm^{-3} total ionic strength.
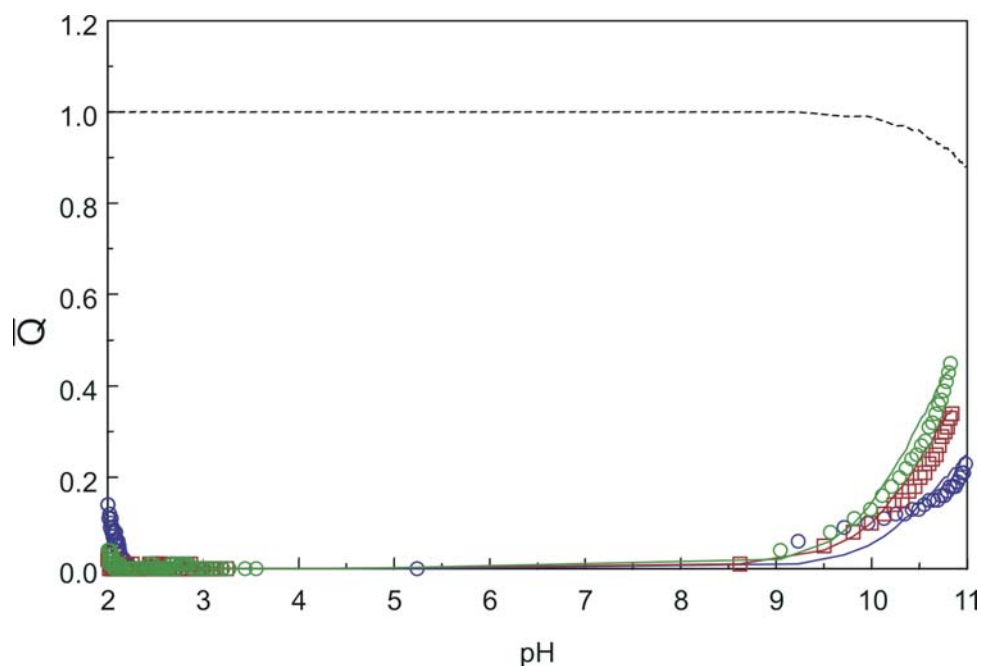
Figure 3 Experimental (symbols) and modelled (lines) deprotonation curves for complexation of BIU by Ca(II). The dashed line is the n-curve, representing the protonation state of the ligand in the absence of the metal ion. The titrations are represented by: (○) 0.001001 mol dm^{-3} BIU, 0.000972 mol dm^{-3} Ca(II) and 0.009921 mol dm^{-3} HCl; (□) 0.002001 mol dm^{-3} BIU, 0.000972 mol dm^{-3} Ca(II) and 0.010079 mol dm^{-3} HCl; (△) 0.003002 mol dm^{-3} BIU, 0.000972 mol dm^{-3} Ca(II) and 0.010084 mol dm^{-3} HCl; *versus* 0.0500 mol dm^{-3} NaOH in 0.10 mol dm^{-3} NaCl at 25 °C and 0.15 mol dm^{-3} total ionic strength.

$\overline{Z}_M = 1$, indicating one ligand molecule per metal ion, as modelled. HL predominates for the pH range 4 to 10 for DMBG and BIU. Therefore, if a MLH complex would form (M + LH → MLH), there would be no release of protons and potentiometry would not detect this complexation reaction: a $\overline{Q}$ of zero would be expected. Another technique, such as potentiometric titration with the use of appropriate ion-specific electrodes or spectroscopy, is needed to confirm this. The $\overline{Q}$ curves (Fig. 3) move towards the $\overline{n}$ (the protonation state of the ligand in the absence of the metal ion) curve at a high pH of 11, indicating that an ML-type complex forms. The species distribution curves reflect only the ML complex predominating at pH > 10. It is viewed as unlikely that the metal ions would be complexed at a lower pH by BIU without deprotonation taking place, as this would entail the loss of the extra stability afforded to the ligand by the amide effect. It was therefore assumed that no competition from Mg(II) and Ca(II) for the ligand is to be expected at the physiological pH of 7.4. To see whether the presence of an MLH complex would detrimentally affect the complexation of these ligands in blood plasma, an analogue (*viz.* BIG) was studied (see Supplementary Material).

The biguanide complexes of metal ions (transition metals) form as charged or uncharged metal biguanides according to the ligand basicity.[20] Stability constants and/or crystal structures of DMBG-alkaline earth metal complexes have not been reported in the literature. The reported data are discussed in Section 3.1.7, indicating that, although mostly ML$_2$ species form, ML species can also exist with transition metal complexation.

The BIU molecule can adopt either the *cis*- or the *trans*-configuration. Spectroscopic studies[21] showed that ML$_2$ species form with Mg(II) and Ca(II), BIU is bound to Mg(II) as a bidentate ligand via the two oxygen atoms in a *cis* configuration (also mentioned for crystal structures of Zn(II) and Ni(II)), while the monodentate *trans*-configuration, with an intramolecular hydrogen bond was found for Ca(II) (also mentioned for Hg(II) and Cd(II)). However, potentiometric studies reported that the

ML species is formed when M=Zn(II), Cd(II) and Hg(II), whereas ML and ML$_2$ are formed when M=Cu(II) and Ni(II).[18] The spectroscopic or crystallographic studies and potentiometric studies differ in the species that can form, which are also found in this study when comparing with predominantly crystallographic studies in the literature.

Metal complexes of ITB can react in either of their tautomeric forms to form an inner-metal complex of different structures, depending on the nature of the metal. The reported data again are limited to ITB-transition metal complexation (see Section 3.1.7).

In Mg(II)-ITB, the MLOH species are formed, where the proton is lost from the ligand, presumably from the thiourea part of the molecule, since log K$_{MgOH}$ = 2.58 < log K$_{MLOH}$ = 5.92, which implies that the proton is not lost by the coordinated water (if the proton was released by the coordinated water then the constant of the complex should be higher than or similar to that of the metal hydroxide and is recorded as MLH$_{-1}$). The deprotonation curves (Fig. 4) show that $\overline{Q}$ rises above $\overline{n}$ (= $\overline{Z}_H$), indicating that more protons are detected in the system than expected from the ligand and confirming that the ligand is deprotonated. Backfanning is also found with the $\overline{Z}_M$ curves that indicate that the hydrolysis species is present.[10] At pH 4.5 to pH 7 the ligand releases a proton while $\overline{Q}$ remains at 0, indicating that no protons are released from the metal ion centre on complexation. Therefore, the equation can be written as

$$M + LH - H \rightarrow ML,$$

although one would suspect that the $\overline{Q}$ will increase to 1 from pH 7 onwards. This does not happen, and it is therefore questionable whether MgL is found at physiological pH, while MgLH$_{-1}$ formed from pH 8 onwards. For Ca(II)-ITB, the $\overline{Q}$ curves show that little or no complexation occurs at pH > 7, implying that little Ca(II) is complexed at physiological pH by ITB and limiting the mobilization of Ca(II) that could lead to side effects. The ML species was not found for Ca(II)-ITB, probably due to the very weak or non-existent complexation of Ca(II) by ITB at
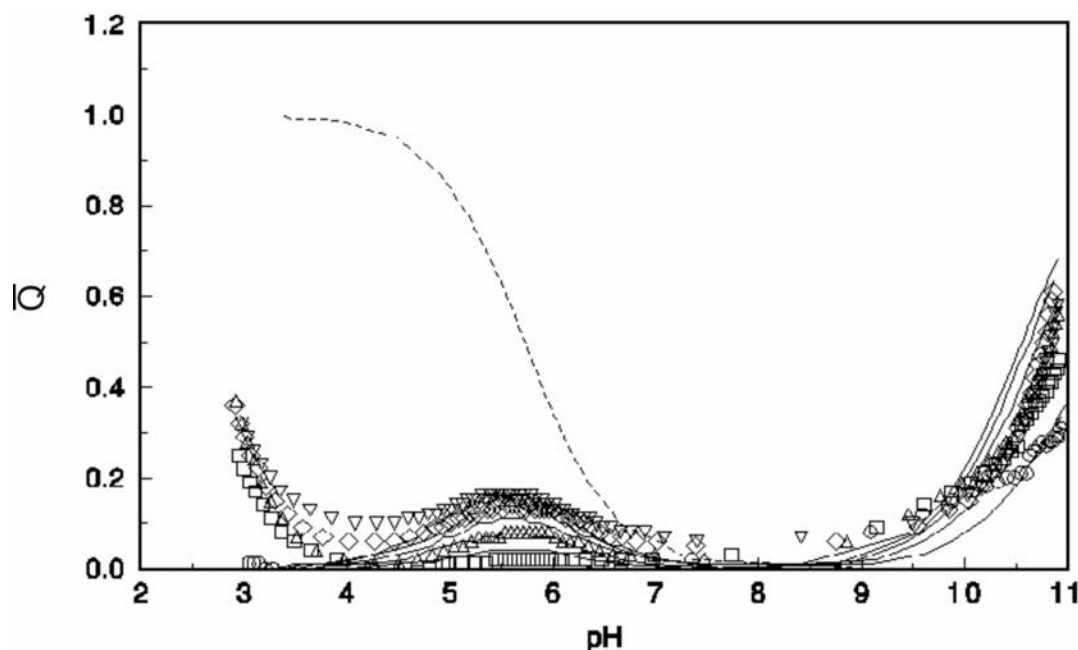
Figure 4 Experimental (symbols) and modelled (lines) deprotonation curves for complexation of ITB by Mg(II). The dashed line is the n-curve, representing the protonation state of the ligand in the absence of the metal ion. The five titrations are represented by: (○) 0.0009935 mol dm^{-3} ITB, 0.0009904 mol dm^{-3} Mg(II) and 0.009543 mol dm^{-3} HCl; (□) 0.0019871 mol dm^{-3} ITB, 0.0009904 mol dm^{-3} Mg(II) and 0.0093807 mol dm^{-3} HCl; (△) 0.0029807 mol dm^{-3} ITB, 0.0009904 mol dm^{-3} Mg(II) and 0.0093807 mol dm^{-3} HCl; (◇) 0.0040014 mol dm^{-3} ITB, 0.0009904 mol dm^{-3} Mg(II) and 0.0094647 mol dm^{-3} HCl; (▽) 0.0050017 mol dm^{-3} ITB, 0.0009904 mol dm^{-3} Mg(II) and 0.0094647 mol dm^{-3} HCl; *versus* 0.0500 mol dm^{-3} NaOH in 0.10 mol dm^{-3} NaCl at 25 °C and 0.15 mol dm^{-3} total ionic strength.

the intermediate pH values. Ca(II) only starts to complex at pH > 8.5 in the form of an MLH_{-1} complex. Again, one cannot see the formation of ML from potentiometry as the L species predominates at pH = 7.4 and no protons are released. To see whether the effect of an ML complex would detrimentally affect the complexation of these ligands in blood plasma, analogues (carbamic acid, β-alanine and N-acetylthiourea) were studied with the ECCLES program (see Supplementary Material).

The $\overline{Q}$ curves for Mg(II) and Ca(II) complexation by CBIG show that no protons are released per metal ion in the pH 2 to pH 10 range, while the protonation curve ($\bar{n}$) moves from LH_2 to LH, showing the possibility of MLH and MLH_2 forming as modelled. No complexes can be found by potentiometry for pH 6 to pH 10 with the predominant L-species. The formation curves show that $\overline{Z}_M$, which is equal to the number of ligands bound per metal ion, is 0, indicating that no complexes form. At normal blood plasma pH 7.4, $\overline{Q}$ and $\bar{n}$ = 0, no protons are released from the ligand or metal ion, thus confirming that no complexation takes place. This means that CBIG will not mobilize Ca(II) and Mg(II) in blood plasma.

3.1.7. *Zn(II)-DMBG, BIU, ITB, CBig Systems, Ni(II)-ITB System and Cu(II)-CBig System*

The reaction systems of Zn(II) with DMBG and BIU show similar $\overline{Q}$ and $\overline{Z}_M$ curves. Backfanning of the $\overline{Z}_M$ curves and the $\overline{Q}$ curves that move above the $\bar{n}$ value indicate the presence of $ML(OH)_x$ type complexes. DMBG log K_{ZnOH} = 5 < log K_{MLOH} = 12.57 and BIU log K_{ZnOH} = 5 < log K_{MLOH} = 12.79, thus MLH_{-1}-species form (as explained in Section 3.1.6).

For DMBG-metal complexes (for example with Cu(II) and Ni(II)), it is assumed that the less basic of the two groups in the N^1 and/or N^5 positions coordinates with the metal ion. The metal replaces the H on the imino (=NH) group and is linked to the nitrogen atom of the $N(CH_3)_2$ group.[1] Crystal structure studies show π-electron delocalization over all the nitrogen atoms,

resulting in sp^2 hybridization of the amine groups with no lone pair electrons that can direct to the transition metals, indicating imine coordination rather than amine coordination.[22,23] Complexes containing only one molecule of the ligand with Cu(II) and not with Ni(II) have been observed in aqueous solutions with the progressive addition of acid. They are only stable in acid solution within certain limits and are decomposed with excess acid.[1]

The transition metals form neutral species with ITB that are susceptible to precipitation. Data points were deleted where precipitation occurred. The $\overline{Q}$-curves obtained for Ni(II) show that the $\bar{n}$ curve is below the $\overline{Q}$-curve from pH 6.5 and at pH 8 $\bar{n}$ = 0 and $\overline{Q}$ = 2, thus two protons are lost by the ligand due to complexation forming NiL_2H_{-2}. The hydroxy species is also confirmed with the backfanning of the formation curves (Fig. 5). A yellow-orange precipitate forms from pH 8 onwards, similar in colour to that of a reported Ni(II)-ITB compound.[1] From literature crystal structure data, the Ni complex resembles the complexes of Ni(II) guanylurea and Ni(II) biguanide as ML_2 species. In this structure, the hydrogen atom of an imino group (=NH) in each ITB molecule is replaced by the metal ion and one of the amino groups (-NH_2) is also linked to the metal ion by a coordinate bond. The copper-ITB complex, however, contains ML species with the metal ion linked by a metal-sulphur bond and amino coordinate bond.[1] It is thus concluded that Ni(II) (72 % according to species distribution curves) is complexed as NiL_2H_{-2} at physiological pH 7.4. According to the deprotonation curves, the modelled complex ZnL_2H_{-2} is found, although the $\overline{Q}$ and $\overline{Z}_M$ fits are not as good as for Ni(II). This can be attributed to the precipitate not being visible in the beginning.

The $\overline{Q}$ curves for Cu(II)-CBIG show at pH 5 to pH 7 that $\bar{n}$ = 0 and $\overline{Q}$ = 1, indicating that hydroxy species are formed. This is also confirmed by the backfanning of the formation function curves. The predominant CuLOH species is shown to reach 100 % at pH 7.4 in the species distribution curves. No data were
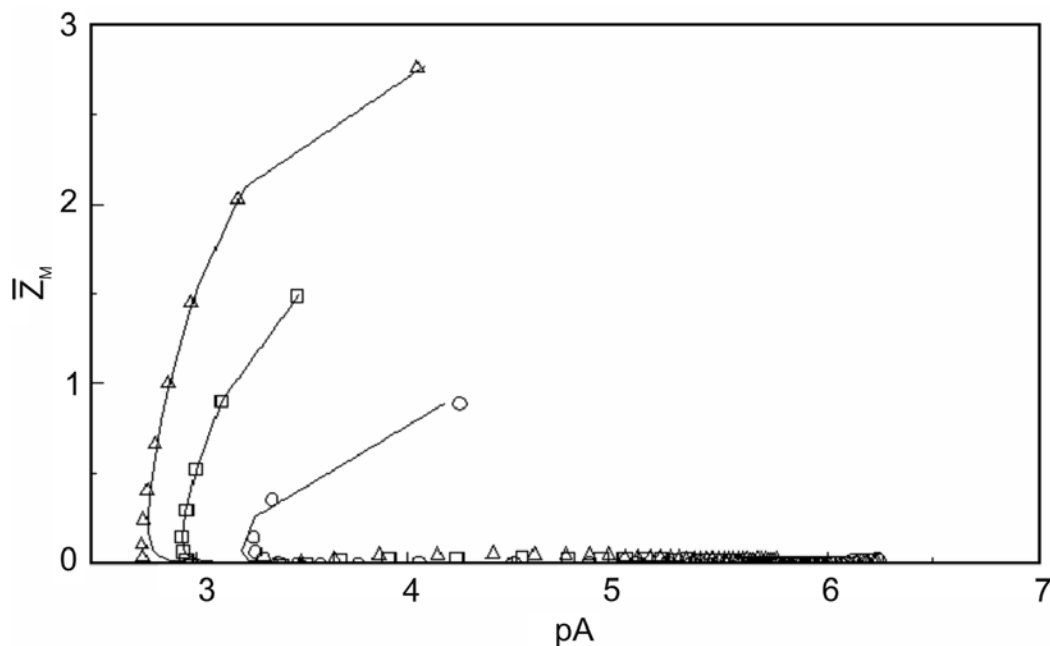
Figure 5 Experimental (symbols) and modelled (lines) formation curves for complexation of ITB by Ni(II). The titrations are represented by: ($\bigcirc$) 0.000993 mol dm^{-3} ITB, 0.0010341 mol dm^{-3} Ni(II) and 0.0096889 mol dm^{-3} HCl; ($\square$) 0.0019871 mol dm^{-3} ITB, 0.0010341 mol dm^{-3} Ni(II) and 0.0096730 mol dm^{-3} HCl; ($\triangle$) 0.0029807 mol dm^{-3} ITB, 0.00096889 mol dm^{-3} Ni(II) and 0.0096889 mol dm^{-3} HCl; *versus* 0.0500 mol dm^{-3} NaOH in 0.10 mol dm^{-3} NaCl at 25 °C and 0.15 mol dm^{-3} total ionic strength.

recorded above pH 7, since precipitation formed.

Owing to precipitate formation at ligand to metal ratios used in potentiometric titrations, the formation constants for Zn(II) complexation by CBIG were measured by polarography (Fig. 6). The polarographic titrations were performed at fixed pH values of about 5. The refinement of the data indicated the presence of ML, for which the stability constant obtained was 7.191 (01).

3.1.8. *Ca(II)- and Mg(II)-DMSA Systems*

$\overline{Q}$ and $\overline{Z}_M$ curves for Ca(II) and Mg(II) reaction systems with DMSA were similar. The deprotonation curves ($\overline{Q} = 0.5$) show that one proton is lost per two metal ions, while one and two protons are bound to a ligand, indicating M_2L and M_2LH species. At about pH 8.5, the number of protons lost per metal ion is equal to the number of protons bound per ligand and thus an ML

species is possible. This is also confirmed by the formation curves that approach 1, indicating one ligand per metal ion. The species distribution curves (Fig. 7) show the complexes suggested by the $\overline{Q}$ curves. At pH 7.4, M_2L and ML complexes are predominant, meaning that the Ca(II) and Mg(II) in the blood plasma may be mobilized by the DMSA. The stability constants of Mg(II) < Ca(II) are contrary to the Irving-Williams series, but this tendency was also found by Martell for di- and tri-carboxylic acids.[24]

3.1.9. *Cu(II)-DMSA System*

The deprotonation curves for the complexation of Cu(II) by DMSA show that $\overline{Q} = 0.5$ at pH < 6, implying that one proton is lost per two metal ions and $\overline{n}$ moves from 1 to 2, which implies that one or two protons are bound to the ligand, which
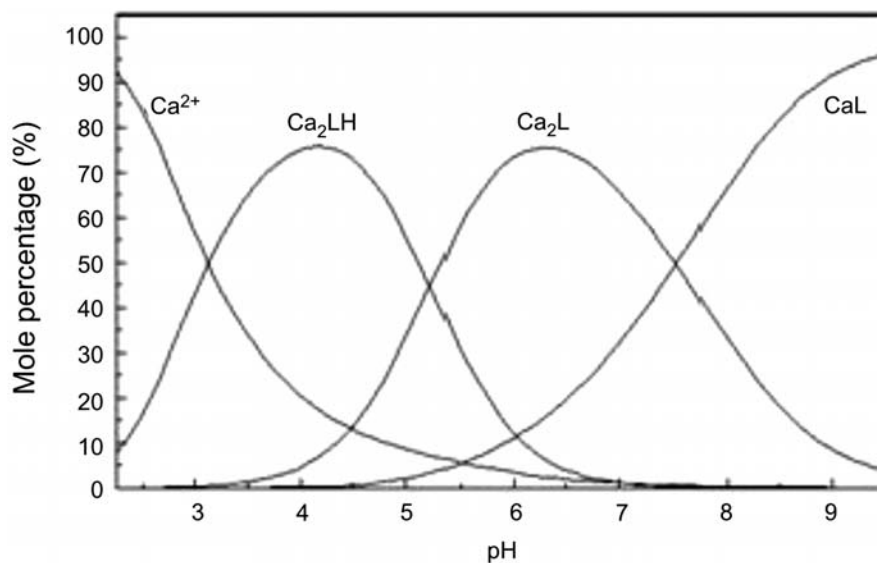

Figure 6 Species distribution curves for the Ca(II) complexation by DMSA at 25.0 ± 0.1 °C in 0.15 mol dm^{-3} NaCl. The curves were generated from the M:L = 1:2; [DMSA] = 0.001998 mol dm^{-3}, [Ca(II)] = 0.000972 mol dm^{-3}.
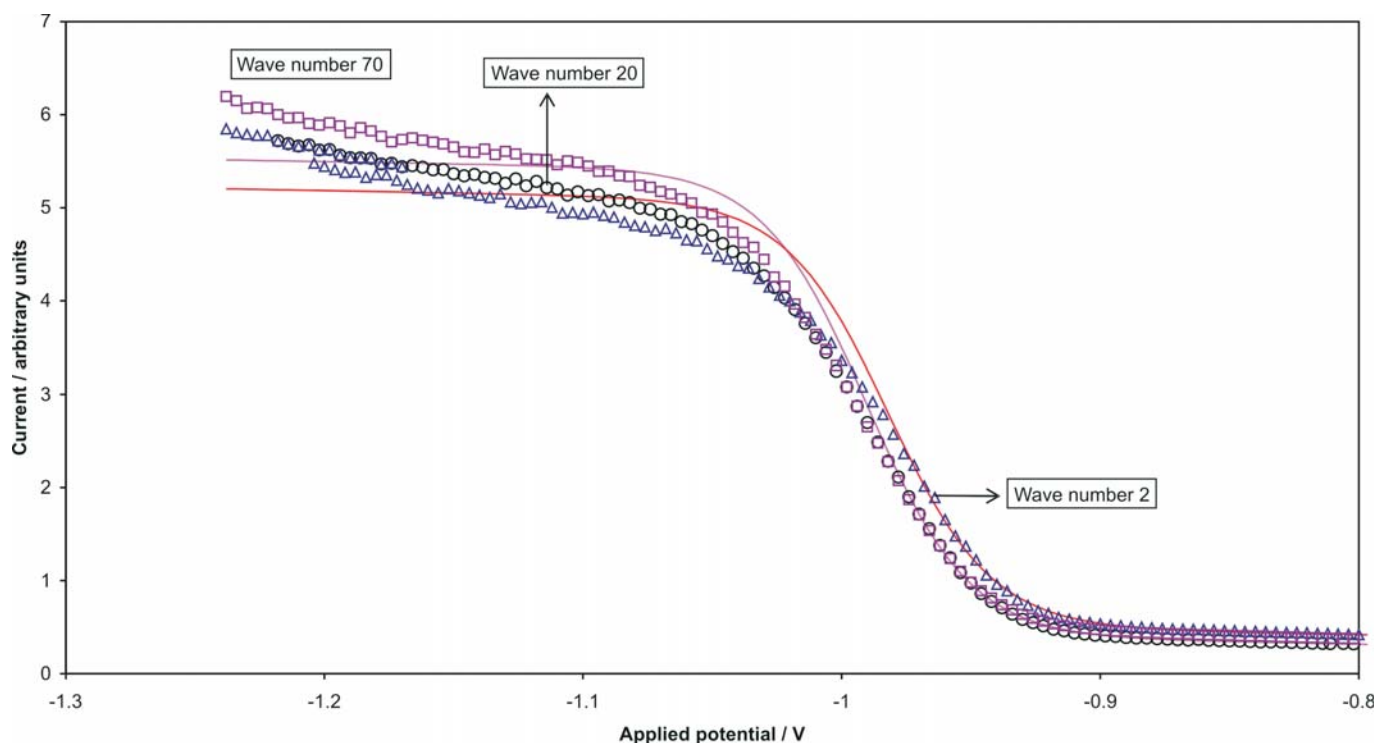
Figure 7 Plot of experimental DC polarograms (points) and computed reduction currents at specific pH values for the ZnCBIG system (ligand titration).

respectively leads to the M_2L and M_2LH species. At pH 6.5 $\overline{Q} = \overline{n}$, which indicates that ML is possible. Hydroxy species, MLOH and $ML(OH)_2$, are also found, since $\overline{Q}$ moves above the $\overline{n}$ curve, and this is confirmed by the backfanning of the formation function curves. The species distribution curves show that CuL, CuLOH and $CuL(OH)_2$ are present at pH 7.4, meaning that Cu(II) could be mobilized by DMSA in blood plasma.

3.1.10. *Sn(II)-DMBG System*

The modelled SnDMBG(OH) complex (Table 1) is evident from the backfanning of the $\overline{Z}_M$ curves and the $\overline{Q}$ curves that

move above the $\overline{n}$. Since DMBG log $K_{SnOH} = 9.59 < $ log $K_{MLOH} = 20.91$ and BIU log $K_{ZnOH} = 5 < $ log $K_{MLOH} = 12.79$, the proton was released by the coordinated water MLOH-species form. The species distribution curve (not shown) indicates 25 % $Sn(OH)_2$ is present at pH 7.4, which is responsible for the precipitation observed during the titrations. It is therefore expected that the SnDMBG(OH) complex is weak at physiological pH.

3.2. ECCLES Modelling

The blood plasma speciation of the ligands was determined by ECCLES under actual clinical conditions, with a representative
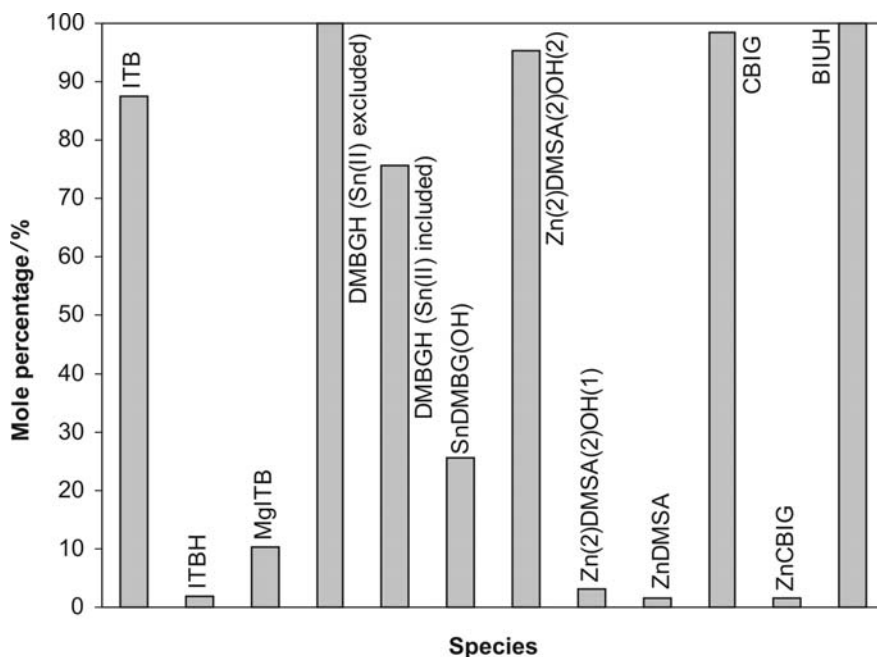

Figure 8 Speciation of ligands in normal blood plasma (pH 7.4 and concentrations of ligands: 5.0×10^{-5} mol dm^{-3} for DMBG, 7.3×10^{-5} mol dm^{-3} for BIU, 6.3×10^{-5} mol dm^{-3} for ITB, 4.3×10^{-5} mol dm^{-3} for CBIG and 1.4×10^{-5} mol dm^{-3} for DMSA) .
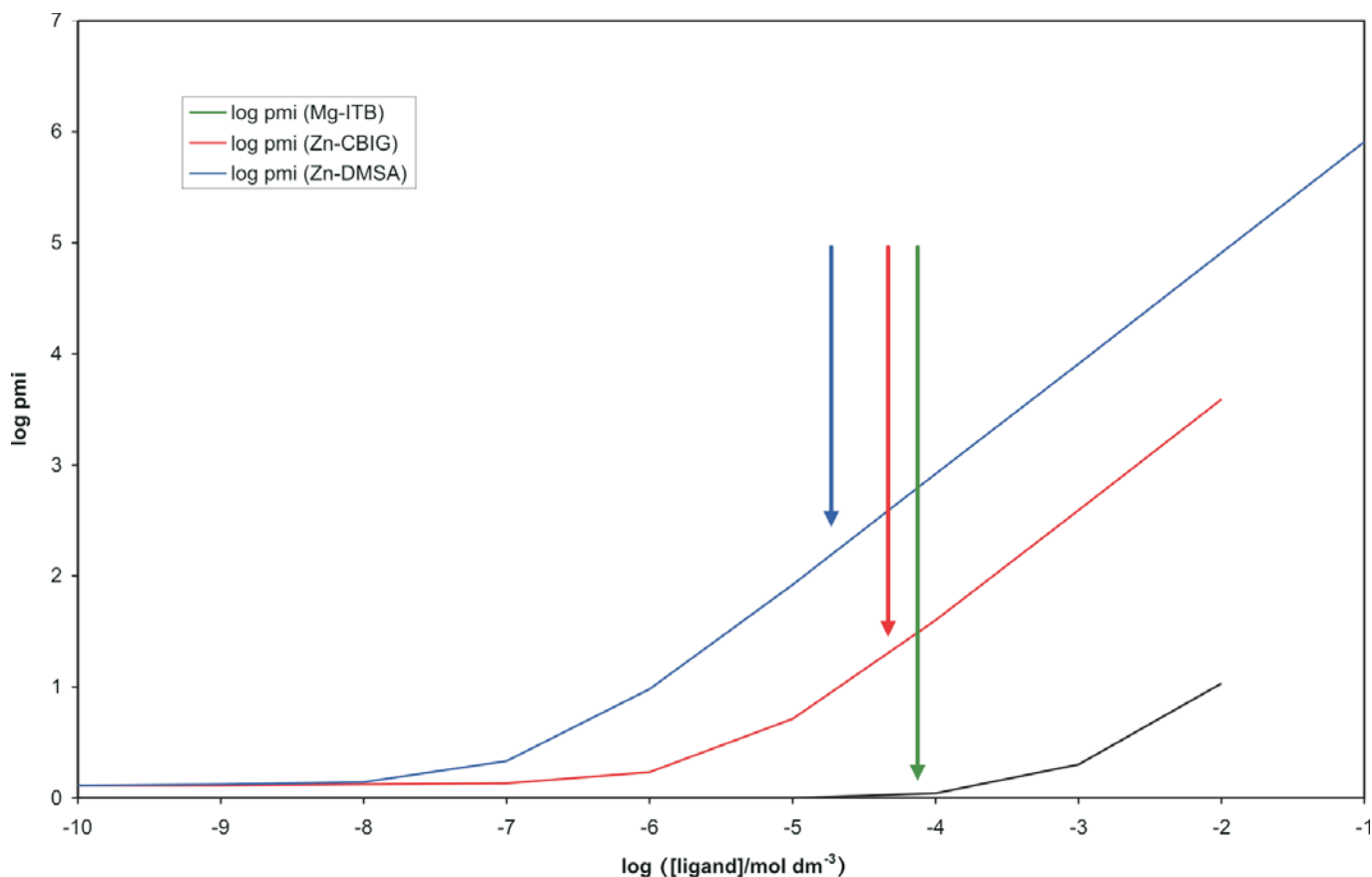
Figure 9 Plasma mobilization index (p.m.i.) curves for blood plasma metal ions versus ligand concentration with significant contribution. The arrows indicate the typical ligand concentrations used clinically.

ligand concentration for the respective ligands. The speciation of the ligands (Fig. 8) in normal blood plasma showed that:

i. DMBG (without Sn(II)), BIU and CBIG have virtually no interaction with blood plasma metal ions, while ITB experiences some complexation with Mg(II). A significant (although not totally defining) change occurs in the species distribution of DMBG, if Sn(II) is included. This implies that ~25 % of the ligand stays bound to Sn(II), as was already the case in the formulation pre-injection, and will not mobilize other blood plasma metal ions. If one considers that the low stoichiometric amount of Tc in the formulation of Sn(II) will not reduce the number of labelled DMBG sites, and that the other blood plasma ligands and metal ions will not do so either, it may be expected that the labelling of ^{99m}Tc DMBG will not be adversely influenced and that the biodistribution seen in animals will be that of the ligand. 6.9 % of Sn(II) in the formulation is bound to DMBG, while the rest is distributed to other blood plasma ligands, which is in line with the normal biodistribution of SnCl$_2$.

ii. DMSA is the only ligand that has considerable binding to blood plasma metal ions. Its speciation calculations show that almost 100 % of the ligand is bound by Zn(II). As the complexation by Zn(II) is very strong, it is not expected that Sn(II) will alter the species distribution of DMSA in blood plasma. It is therefore expected that the biodistribution studied in animals with ^{99m}Tc-DMSA will be that of Zn(II)-DMSA (more particularly Zn$_2$(DMSA)$_2$(OH)$_2$) and not DMSA alone. It is shown that DMSA substantially mobilizes Zn(II) metal ions (Fig. 9), which might prompt one to give such patients Zn(II) supplements.

4. Conclusion

It was shown for DMBG, BIU and ITB that metals will not be mobilized significantly at the physiological pH and it can be predicted that no serious side effects due to metal ion mobilization will be found. CBIG causes some side effects, as Zn(II) is mobilized, although not to the same extent as found for DMSA. In order to verify the theoretical results, biodistribution tests on vervet monkeys should be performed.

References

1 P. Ray, *Chem. Rev.,* 1962, **62**, 313–359.
2 *http://www.medcyclopaedia.com* Physics, techniques and procedures: Radionuclide renal imaging. General Electric Company 1997–2007, GE Healthcare. Accessed 2 August 2004.
3 *http://www.gpnotebook.co.uk* General practice notebook – a UK medical reference on the World Wide Web, Static renal scintigraphy, Oxbridge Solution Ltd., 2007. Accessed 2 August 2004.
4 M. Neves, I. Dormehl, E. Kilian, W. Louw, K. Lalaoui and J.J. Pedroso de Lima, *Nucl. Med. Biol.,* 2000, **27**, 593–597.
5 M. Neves, L. Gano, M. João Ribeiro, A.C. Santos, A. Marchi, C. Sawas-Dimopolou and J.J. Pedroso de Lima, *Nucl. Med. Biol.,* 1999, **26**, 79–83.
6 A. Marchi, M. Neves, L. Marvelli, M. Cattabriga, R. Rossi, V. Bertolasi and V. Ferretti, *Technetium, Rhenium and Other Metals in Chemistry and Nuclear Medicine* (M. Nicolini and U. Mazzi, eds.), vol. 5, 5th edn., SG Editoriali, Padova, Italy, 1999, pp. 271–275.
7 M. Neves and R. Fautso, *Nucl. Med. Biol.,* 1999, **26**, 85–89.
8 A. Marchi, L. Marvelli, M. Cattabriga, R. Rossi, M. Neves, V. Bertolasi and V. Ferretti, *J. Chem. Soc., Dalton Trans.,* **1999**, 1937–1943.
9 S.D. Larsen, M.A. Connell, M.M. Cudahy, B.R. Evans, P.D. May, M.D. Meglasson, T.J. O'Sullivan, H.J. Schostarez, J.C. Sih, F.C. Stevens, S.P. Tanis, C.M. Tegley, J.A. Tucker, V.A. Vaillancourt, T.J. Vidmar, W. Watt and J.H. Yu, *J. Med. Chem.,* 2001, **44**, 1217–1230.

10 J. R. Zeevaart, N.V. Jarvis and W.K.A. Louw, *J. Inorg. Biochem.,* 2001, **83,** 57–65.

11 J. R. Zeevaart, W.K.A. Louw, Z.I. Kolar, J.M. Wagener, N.V. Jarvis and R.A.M.J. Claessens, *J. Radioanal. Nucl. Chem.,* 2003, **257**, 83–91.

12 J. R. Zeevaart, D.R. Jansen, M.F. Botelho, A. Abrunhosa, C. Gomes, L. Metello, Z.I. Kolar, G.C. Krijger, W.K.A. Louw and I.C. Dormehl, *J. Inorg. Biochem.,* 2004, **98**, 1523–1530.

13 P.M. May, K. Murray and D.R. Williams, *Talanta,* 1985, **32**, 483–89.

14 P.M. May, P.W. Linder and D.R. Williams, *J. Chem. Soc., Dalton Trans.,* 1977, 588–95.

15 A.E. Martell and R.M. Smith (eds), NIST Standard Reference Database 46, Version 8.0, Gaithersburg, MD 20899, USA, 2003.

16 J. R. Zeevaart and S. Olsen, *Appl. Radiat. Iso.,* 2006, **64**, 812–814.

17 J. R. Zeevaart, W.K.A. Louw, E. Kilian and I. Cukrowski, ^{99m}Tc labelled biguanide derivatives: chemical speciation modelling thereof and evaluation in vervets, submitted to *J. Inorg. Biochem.*

18 R.M. Sanyal, P.C. Srivastava and B.K. Banerjee, *J. Inorg. Nucl. Chem.,* 1975, **37**, 343–347.

19 R.D. Hancock and A.E. Martell, *Chem. Rev.,* 1989, **89**, 1875–1914.

20 R.C. Mehrotra, *Comprehensive Coordination Chemistry* (G. Wilkinson, ed.), vol. 2, Pergamon Press, Elmsford, NY, USA, 1987, pp. 269–291.

21 M. Goodgame and I. Hussian, *Inorg. Chim. Acta,* 1989, **160**, 183–188.

22 R.K. Ray and G.B. Kaufman, *Inorg. Chim. Acta,* 1990, **173**, 207–214.

23 R.K. Ray and G.B. Kaufman, *Inorg. Chim. Acta,* 1990, 174, 257–262.

24 A.E. Martell and R.M. Smith, *Critical Stability Constants,* vol. 3, Plenum Press, New York, USA, 1977.

25 A.E. Martell and R.M. Smith, *Critical Stability Constants,* vol. 1, Plenum Press, New York, USA, 1974.